HiSST: 2nd International Conference on
High-Speed Vehicle Science & Technology
11-15 September 2022, Bruges, Belgium

Thermal non-equilibrium modeling for ablative gas-surface interaction

Michele Capriati[*1], *Georgios Bellas Chatzigeorgis*[1], *Alessandro Turchi*[1], *Bernd Helber*[1], *Thierry E. Magin*[1]

Abstract

The strong shock experienced by a spacecraft entering the atmosphere leads to the formation of a highly reactive boundary layer that interacts with its surface through chemical reactions and heat exchange. From a numerical prospective, these gas-surface interactions can be modeled as a boundary condition that allows to compute macroscopic properties, such as temperature and recession rates. Mass and energy conservation is imposed at the surface. In the present work, an ablative surface was numerically simulated. Since a two-temperature model was employed to describe the flowfield, a surface vibrational energy balance was derived. It was compared with two extreme cases: surface in thermal equilibrium and surface vibrationally adiabatic. Results shows that considering surface vibrational energy relaxation has an important impact on the surface temperature and on the recession rate. Furthermore, it suggests a possible high internal excitation close to the surface.

Keywords: *Gas-surface interaction, surface-balance, nitridation, ablation, thermal non-equilibrium.*

Nomenclature

Latin

h – Specific enthalpy [J/kg]
j – Diffusion flux [kg/m^{2}s]
m – Particle mass [kg]
n – Normal to the surface
$\mathcal{N}$ – Number flux [1 / m^{2}s]
p – Thermodynamic pressure [Pa]
s – Recession rate [μm /s]
S – Source term
T – Temperature [K]
u – Mixture velocity [m/s]

Greek

α – Collisional efficiency
β – Energy accommodation
γ – Reaction probability
ϵ – Emissivity
λ – Thermal conductivity [W/kgK]
ρ – Density [kg/m^3]
σ – Stefan-Boltzmann constant [W/m^{2}K^4]
ω – Chemical production [kg/m^{2}s]

Superscripts

$\mathcal{T}$ – Translational
$\mathcal{V}$ – Vibrational

Subscripts

g – Gas
s – Surface
env – Environment

1. Introduction

In the hypersonic regime that occurs during spacecraft atmospheric entry a shock is generated; across it the gas dissociates into reactive atoms, which diffuse through the Boundary Layer (BL) and interact with the surface [1]: it has to be equipped with a Thermal Protection System (TPS) to preserve its mechanical integrity [2]. The resulting Gas-Surface Interaction (GSI) includes several types of chemical reactions (most importantly recombination, oxidation, nitridation and sublimation) and heat exchanges. The GSI is strongly coupled with the gas phase, thus, from a numerical point of view, it has to be modeled as a boundary condition, that, coupled with a CFD code, allows the user to predict macroscopic properties, such as surface temperature and recession rate. The most common approach is to impose, on an infinitesimal volume containing both the gas and the surface, a mass balance for each species in the mixture and an energy balance for each temperature in the thermodynamic model. The GSI' s physics

[1] *von Karman Institute for Fluid Dynamics, Sint-Genesius-Rode, B-1640, Belgium, michele.capriati@vki.ac.be*

can be handled directly by the CFD software, but it can be more convenient to have an external library providing a state-of-the-art model easy to be interfaced. In this study, it was used and expanded the GSI module of the open source library MUTATION^{++} [3, 4].
Generally, the gas-surface layer is assumed to be in thermal equilibrium, forcing the vibrational surface temperature to be equal to the translational one and no vibrational energy balance is needed.
Anyway, experimental campaigns [5] and numerical simulations [6] conducted to study nitrogen heterogeneous recombination suggested that products may escape the surface with excited internal energy levels, leading the above assumption not to be regarded valid under all the circumstances.
Furthermore, an experimental campaign conducted at the von Karman Institute to study low pressure surface nitridation reveals high vibrational energy levels in the reactive BL [7]. Moving from these motivations, an energy balance for vibrational energy at the surface was derived to investigate whether this thermal non-equilibrium arises from the GSI.
The new model was coupled with an in-house CFD software solving dimensional reduced, chemical reacting, two-temperatures Navier-Stokes equations [8]. It provides the solution along the stagnation line of the body and on the surface stagnation point.
The above-mentioned experimental campaign was used as input for the simulations. Three different vibrational boundary conditions were used to investigate the impact of the surface thermal non-equilibrium on its macroscopic properties: the developed vibrational balance, a gas-surface layer in thermal equilibrium and a surface vibrationally adiabatic.

2. Methodology

2.1. Governing equation and flow solver

The flow is a gas mixture of $\mathrm{n_S}$ chemical reacting species in thermal non-equilibrium, treated according to Park two-temperature model[9] that considers the rotational energy mode to thermalize with the translational one ($T^{\mathcal{T}} = \mathcal{T}^{\mathrm{R}}$) and the electrons/electronic modes with the vibrational one ($T^{\mathcal{V}} = T^{\mathrm{E}} = T^{\mathrm{EL}}$). This last mode will be referred to, from now on, as vibrational one.
The 2 temperatures, chemical reactive Navier-Stokes equations are:

$$\frac{\partial \rho_{\mathrm{i}}}{\partial t} + \nabla \cdot (\rho_{\mathrm{i}} \mathbf{u} + \mathbf{j}_{\mathrm{i}}) = \dot{\omega}_{\mathrm{i}} \quad \forall \mathrm{i} \in [1, \mathrm{n_S}], \tag{1}$$

$$\frac{\partial \rho_{\mathrm{i}} \mathbf{u}}{\partial t} + \nabla \cdot (\rho_{\mathrm{i}} \mathbf{u} \cdot \mathbf{u} + p\bar{\bar{\mathrm{I}}} + \bar{\bar{\tau}}) = \mathbf{0}, \tag{2}$$

$$\frac{\partial \rho E}{\partial t} + \nabla \cdot (\rho \mathbf{u} H + \bar{\bar{\tau}} \mathbf{u} + \mathbf{q}) = 0, \tag{3}$$

$$\frac{\partial \rho e^{\mathcal{V}}}{\partial t} + \nabla \cdot (\rho \mathbf{u} e^{\mathcal{V}} + \mathbf{q}^{\mathcal{V}}) = \Omega^{\mathcal{V}\mathcal{T}} + \Omega^{\mathrm{C}\mathcal{V}} + \Omega^{\mathrm{E}\mathcal{T}} - \Omega^{\mathrm{I}}. \tag{4}$$

Symbol ρ_{i} is the partial density of species i, $\mathbf{u}$ is the mass-averaged mixture velocity, $\mathbf{j}_{\mathrm{i}}$ the diffusion mass flux of species i, $\dot{\omega}_{\mathrm{i}}$ its chemical production/destruction rate, p, the thermodynamic pressure of the mixture, $\bar{\bar{\tau}}$, the viscous stress tensor, E, the total energy, $H = E + p/\rho$, the total enthalpy, and $\mathbf{q}$, the total heat flux. The two-temperature thermodynamic state is computed according to the rigid rotor harmonic oscillator assumption. Transport proprieties are computed using the Stephan-Maxwell model for diffusive fluxes and the Chapman-Enskog formulation for viscosity and thermal conductivity [10].
The right-hand side of the vibrational energy conservation, eq. 4, represents the energy transfer between the translational and the vibrational mode. The first term is the energy exchange by collisions between the vibrational and the translational mode and can be modelled using the Landau-Teller formulation [11]:

$$\Omega^{\mathcal{V}\mathcal{T}} = \sum_{\mathrm{i} \in \mathcal{M}} \rho_{\mathrm{i}} \frac{h_{\mathrm{i}}^{\mathcal{V}}(T^{\mathcal{T}}) - h_{\mathrm{i}}^{\mathcal{V}}(T^{\mathcal{V}})}{\tau_{\mathrm{i}}^{\mathcal{V}\mathcal{T}}}, \tag{5}$$

where "$\mathcal{M}$" denotes the set of vibrating molecules and $\tau_{\mathrm{i}}^{\mathcal{V}\mathcal{T}}$ is the characteristic relaxation time. It was computed according to the Millikan and White empirical formula [12] with Park correction [13]. The

second term represents the energy added/subtracted to the vibrational mode due to recombination/dissociation. It was evaluated according to[14]:

$$\Omega^{\mathrm{cv}} = \sum_{\mathrm{i}\in\mathcal{M}} h_{\mathrm{i}}^{\mathcal{V}} \dot{\omega}_{\mathrm{i}}, \tag{6}$$

where $\mathcal{M}$ is the set of molecule created/destroyed by chemical reactions. The third term represents the exchange of energy between free electrons and heavy species; it was also evaluated using a Landau-Teller formulation. The term Ω^{I} can be expressed as:

$$\Omega^{\mathrm{I}} = \sum_{\mathrm{i}\in\mathcal{I}} \Delta h_{\mathrm{i}} \mathcal{R}_{\mathrm{i}}, \tag{7}$$

where $\mathcal{R}_{\mathrm{i}}$ is the rate of progress for the ionization reaction and Δh_{i} is the ionization energy, computed according to [15].
All the used models and energy transfers were computed by means of the MUTATION^{++} library.
The 2T NS system can be dimensionally reduced by means of the stagnation-line theory for axisymmetric problems: the system of equations is firstly reduced in spherical coordinates system (r, θ, ϕ). Exploiting the axial symmetry around r axis, $u_\phi = \frac{\partial}{\partial\phi} = 0$. Applying the separation of variables and letting θ tend to zero allows the problem to be reduced in one dimension; further details can be found in [16].
The system is then implicitly solved after a discretization in a finite volume fashion until convergence to the steady-state. The boundary conditions are imposed by means of ghost cells. In the present study an in-house software [8] for solving reduced NS equations was employed.

2.2. Surface boundary conditions

The present study deals with a non-pyrolyzing ablative surface. Its interaction with the surrounding gas can be expressed in terms of a mass/energy balance on the infinitesimal volume containing both the surface and the gas.
The species mass conservation is sketched in fig. 1: chemistry reactions on the surface generate concentration gradients, driving species diffusion. Furthermore, differently from catalytic surfaces, ablative chemical reactions include material removal with consequent surface gas advection (blowing). Assuming

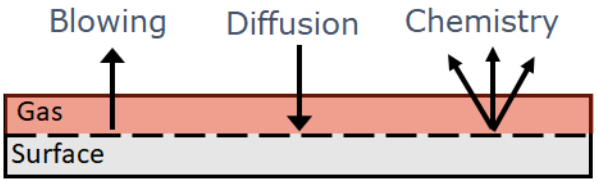

Fig 1. Surface mass balance.

the recession velocity to be negligible compared to the blowing one, the surface mass balance for each species i, in a 1-D frame, reads:

$$\dot{\omega}_{\mathrm{i}} = \rho_{\mathrm{i}} u_{\mathrm{g}} + j_{\mathrm{i}}, \tag{8}$$

where the term $u_{\mathrm{g}} = \sum_{\mathrm{i}=1}^{\mathrm{n_S}} \dot{\omega}_{\mathrm{i}}/\rho_{\mathrm{g}}$ is the advection velocity of the gas at the interface as a result of ablation processes and j_{i} is the diffusion of the species i. The term $\dot{\omega}_{\mathrm{i}}$ is its chemical production and can be computed using phenomenological (such as a γ model [17]) or finite rate chemistry models [18]. In this study the γ model was adopted; according to this, defined the number flux of i species impinging the surface as:

$$\mathcal{N}_{\mathrm{i}} = n_{\mathrm{i}} \sqrt{\frac{k_{\mathrm{b}} T_{\mathrm{S}}}{2\pi m_{\mathrm{i}}}} \tag{9}$$

the probability that a reaction takes place is:

$$\gamma_{\mathrm{i}} = \frac{\mathcal{N}_{\mathrm{i,reac}}}{\mathcal{N}_{\mathrm{i}}} \tag{10}$$

where $\mathcal{N}_{\mathrm{i,reac}}$ is the number flux of species subject to the reaction. A value of γ equal to the unit means that all the species particles are subject to that reaction; when a species is involved in more than a reaction the sum of all its γ should be at maximum equal to the unity. On the other hand, when γ is equal to zero, the reaction does not take place. Provided to know the γ law or value, the chemical source term reads:

$$\dot{\omega}_{\mathrm{i}} = \gamma_{\mathrm{i}} \mathcal{N}_{\mathrm{i}} m_{\mathrm{i}}. \tag{11}$$

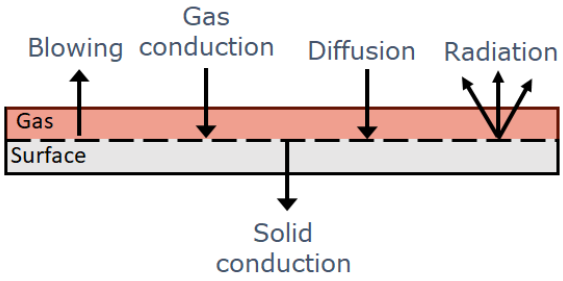

Fig 2. Surface total energy balance.

The surface total energy balance is sketched in fig.2. Assuming steady-state solid conduction[19], it reads:

$$\rho u_{\mathrm{g}} h - \lambda^{\mathcal{T}} \frac{\partial T^{\mathcal{T}}}{\partial n} - \lambda^{\mathcal{V}} \frac{\partial T^{\mathcal{V}}}{\partial n} + \sum_{\mathrm{i}=1}^{\mathrm{n_S}} j_{\mathrm{i}} h_{\mathrm{i}} = S_{\mathrm{rad}}, \tag{12}$$

where the first term on the left side represents the energy advected out from the gas-surface layer, the sum of the second and the third term is the heat conducted from the gas to the surface and the fourth the energy diffused in/out. The term on the right side is the energy radiated by the surface treated as a grey body: $S_{\mathrm{rad}} = \sigma \epsilon_{\mathrm{S}} ((T_{\mathrm{S}}^{\mathcal{T}})^4 - T_{\mathrm{env}}^4)$.
When a multi-temperature model is adopted for the gas-phase, a closure for the vibrational energy is needed. In the present study three different boundary conditions were investigated. The most intuitive and conservative one is to constrains the gas-surface layer to be in thermal equilibrium, thus:

$$T^{\mathcal{V}} = T^{\mathcal{T}}. \tag{13}$$

The second one constrains the surface to be vibrationally adiabatic:

$$\frac{\partial T^{\mathcal{V}}}{\partial n} = 0. \tag{14}$$

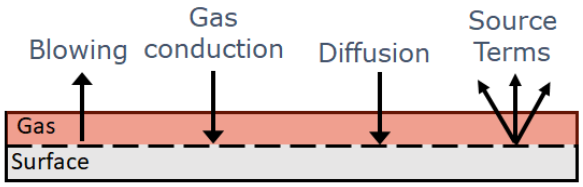

Fig 3. Surface vibrational energy balance.

The third one considers the vibrational equilibrium on the surface, as sketched in fig. 3. It has to allow some species to be produced in an internal excited state (they can than diffuse and be advected out from the gas-surface layer where they can be homogeneously quenched in the gas-phase) and reactants to

diffuse inside in an excited state. Both reactants and products should be also able to be heterogeneously quenched by the surface. The balance reads:

$$\rho u_{\mathrm{g}} h^{\mathcal{V}} - \lambda^{\mathcal{V}} \frac{\partial T^{\mathcal{V}}}{\partial n} + \sum_{\mathrm{i}=1}^{\mathrm{n_S}} j_{\mathrm{i}} h_{\mathrm{i}}^{\mathcal{V}} = S_{\mathrm{s}}^{\mathcal{V}\mathcal{T}} + S_{\mathrm{s}}^{\mathrm{c}\mathcal{V}}. \tag{15}$$

The first term on the RHS is the relaxation of internally excited particles by collision with the surface (heterogeneous quenching). It was derived by adapting the volumetric Landau-Teller gas-gas collisions formulation to gas-surface collisions:

$$S_{\mathrm{s}}^{\mathcal{V}\mathcal{T}} = \sum_{\mathrm{i}=1}^{\mathrm{n_S}} \alpha_{\mathrm{i}} \mathcal{N}_{\mathrm{i}} m_{\mathrm{i}} (h_{\mathrm{i}}^{\mathcal{V}}(T^{\mathcal{V}}) - h_{\mathrm{i}}^{\mathcal{V}}(T^{\mathcal{T}})). \tag{16}$$

Where α_{i} is a sensibility parameter that considers that only the α_{i} fraction of collisional events of the species i leads to a relaxation.
The second term on the RHS is a chemical source term that take into account that not all the reaction energy is accommodated on the surface. To model it, let us firstly multiplying the surface mass balance (eq. 8) for the total and vibrational enthalpy of each species and summing it over all the species, it reads:

$$\rho u_{\mathrm{g}} h + \sum_{\mathrm{i}=1}^{\mathrm{n_S}} j_{\mathrm{i}} h_{\mathrm{i}} = \sum_{\mathrm{i}=1}^{\mathrm{n_S}} \dot{\omega}_{\mathrm{i}} h_{\mathrm{i}}$$

$$\rho u_{\mathrm{g}} h^{\mathcal{V}} + \sum_{\mathrm{i}=1}^{\mathrm{n_S}} j_{\mathrm{i}} h_{\mathrm{i}}^{\mathcal{V}} = \sum_{\mathrm{i}=1}^{\mathrm{n_S}} \dot{\omega}_{\mathrm{i}} h_{\mathrm{i}}^{\mathcal{V}}$$

Plugging them respectively in eq.12 and 15, it follows that:

$$\sum_{\mathrm{i}=1}^{\mathrm{n_S}} \dot{\omega}_{\mathrm{i}} h_{\mathrm{i}} - \lambda^{\mathcal{T}} \frac{\partial T^{\mathcal{T}}}{\partial n} - \lambda^{\mathcal{V}} \frac{\partial T^{\mathcal{V}}}{\partial n} = S_{\mathrm{rad}},$$

$$\sum_{\mathrm{i}=1}^{\mathrm{n_S}} \dot{\omega}_{\mathrm{i}} h_{\mathrm{i}}^{\mathcal{V}} - \lambda^{\mathcal{V}} \frac{\partial T^{\mathcal{V}}}{\partial n} = S_{\mathrm{s}}^{\mathcal{V}\mathcal{T}} + S_{\mathrm{s}}^{\mathrm{c}\mathcal{V}}.$$

Subtracting the two equations one gets the conservation of the translational energy:

$$\sum_{\mathrm{i}=1}^{\mathrm{n_S}} \dot{\omega}_{\mathrm{i}} (h_{\mathrm{i}} - h_{\mathrm{i}}^{\mathcal{V}}) - \lambda^{\mathcal{T}} \frac{\partial T^{\mathcal{T}}}{\partial n} = S_{\mathrm{rad}} - S_{\mathrm{s}}^{\mathcal{V}\mathcal{T}} - S_{\mathrm{s}}^{\mathrm{c}\mathcal{V}}. \tag{17}$$

The first term on the LHS is the reaction energy that is accommodated in the translational mode ($q_{\mathrm{i}}^{\mathcal{T}}$). We now claim that only a β_{i} part of this energy is actually accommodated on the surface, thus:

$$\beta_{\mathrm{i}} = \frac{q_{\mathrm{i}}^{\mathcal{T}}}{\dot{\omega}_{\mathrm{i}} (h_{\mathrm{i}} - h_{\mathrm{i}}^{\mathcal{V}})}. \tag{18}$$

Note that the β coefficient is an adaptation for a 2-temperatures model of the energy accommodation term defined by [5], and that a $(1-\beta)$ quota of the heat flux is transferred into the internal energy modes of the products. The chemical source term reads:

$$S_{\mathrm{s}}^{\mathrm{c}\mathcal{V}} = \sum_{\mathrm{i}=1}^{\mathrm{n_S}} \dot{\omega}_{\mathrm{i}} (1 - \beta_{\mathrm{i}}) (h_{\mathrm{i}}^{\mathcal{V}} - h_{\mathrm{i}}). \tag{19}$$

The α and β parameters relative to each component can be assessed both experimentally (high enthalpy facilities or beam techniques) and numerically (molecular dynamic simulations or quantum-mechanic

calculations). Anyway, in this study a phenomenological approach will be proposed, considering the overall effect of the system. Not having prior information about these parameters, a sensibility analysis was performed in the range [0, 1] for the α parameter and on the two extreme case for the β parameter (0 and 1).
The equilibrium condition (eq. 13) can be retrieved if the LHS of eq. 15 minus the chemical term is negligible compared to the inelastic term, i.e. when there are enough effective collisions ($\alpha\mathcal{N}$) with the surface to restore equilibrium.
The adiabatic condition (eq. 14) is the condition for which we expect the surface to be inert to the vibrational mode. Following this assumption, one can assume no collisions to be efficient ($\alpha = 0$) and find the condition for which the vibrational temperature gradient is zero. It follows that:

$$\beta^* = \frac{\sum_{\mathrm{i}=1}^{\mathrm{ns}} \dot{\omega}_\mathrm{i} h_\mathrm{i}}{\sum_{\mathrm{i}=1}^{\mathrm{ns}} \dot{\omega}_\mathrm{i} (h_\mathrm{i} - h_\mathrm{i}^{\mathcal{V}})}. \tag{20}$$

This is equal to say that the vibrational energy lost due to the reaction is recovered by the (1- β^*) part of the reaction enthalpy channelized into the internal degree of energy. For a value of $\beta \in (\beta^*, 1]$ the vibrational temperature on the surface will be lower than the adiabatic one, for $\beta \in [0, \beta^*)$ it will be higher; provided a value of $\alpha = 0$.
The set of ns + 2 balance equations is solved by means of a Newton method and the surface states (densities, temperatures and advection velocity) is returned to the CFD at each iteration until convergence to steady-state.

3. Simulation input

The model was tested on an experimental campaign conducted in the Plasmatron facility to study low pressure nitridation (1500 Pa). The surface temperature was measured by means of a calorimeter, the recession rate by means of a high-speed camera and the temperatures in the BL with a spectrometer. Four different cases were analyzed, whose relative input conditions at the inlet, as well as the experimental surface temperature and blowing mass flux, are listed in table 1. The mixture considered is a carbon-

Table 1. Simulation input (free stream temperature T and velocity u, surface temperature T_s and mass blowing rate $\dot{m}$), and experimental results.

CASE	$T^{\mathcal{T}} = T^{V}[K]$	u [m/s]	T_S	$\dot{m}[g/m^2 s]$
1	10010	1410	2225	[1.60,4.40]
2	10280	1570	2410	[1.92,3.85]
3	11040	1880	2535	[3.61,5.22]
4	10970	1915	2575	[3.70,5.43]

nitrogen one whose molar fractions at the inlet where find imposing chemical equilibrium. The gas-phase chemical reactions were computed according to the rates in [20].
The ablative surface was modeled by imposing the γ law suggested by [21]:

$$\gamma_{\mathrm{CN}} = 7.91 \cdot 10^{-2} \exp\left(-\frac{5653}{T_\mathrm{S}}\right) \tag{21}$$

A 1-D mesh of 730 points generated using a hyper-tangent function with a stretching factor equal to five was used. The mesh convergence was assessed by increasing of an order of magnitude the wall resolution, and stating that the wall heat flux remained almost unchanged.

4. Simulation results

4.1. Equilibrium and adiabatic condition

In this section the results relative to the equilibrium and adiabatic condition at the surface are presented. When the equilibrium boundary condition (eq. 13) is applied, the translational temperature relaxes

within the thermal boundary layer (fig. 4a, solid line, circle marks) to the surface value predicted by the energy balance; for each case, the value is given on table 2. Being the surface vibrational temperature constrained to be equal to the translational one, it also relaxes within the thermal boundary layer (fig. 4a, dashed line, circle marks), mostly because of gas-phase vibrational heat conduction.
Such a relaxation is absent when the equilibrium constrain is removed. In fact, when the adiabatic boundary condition (eq. 14) is used, internal modes do not undergo any significant relaxation within the boundary layer. The vibrational temperature has firstly a downward trend (fig. 4a, dashed line, diamonds marks): it is a consequence of the vibrational energy lost by electrons collisions with heavy species ($\Omega^{E\mathcal{T}}$). Going toward the surface this effect is smoothed out by the fact that electrons start to recombine with N^+ ions (fig. 4b, dashed line), enhancing nitrogen electronic state and reducing the number of collisions between electrons and heavy species (Ω^{I}). As a consequence, atomic nitrogen diffuses inside the boundary layer in electronic excited state. The two behaviours can be more easily appreciated by looking at fig. 5, where each species enthalpy contribute to the overall energy is shown separately. No substantial difference is observed for the species molar fraction evolution in the boundary layer (fig. 4b). The most remarkable difference is the CN value, due to a different surface temperature involved in the gamma computation, which directly affects CN production.

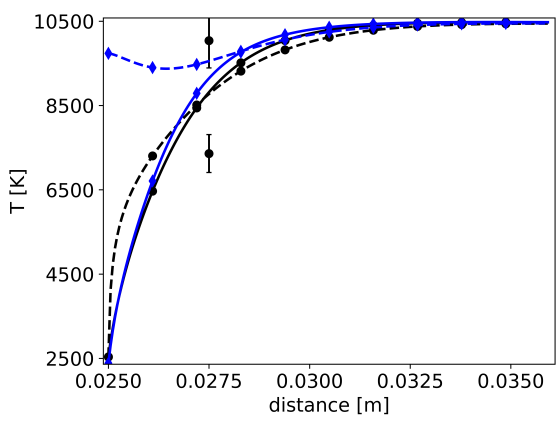

(a) Translational temperature in solid lines. Vibrational temperature in dashed lines. Upper error bar relative to experimental measure of vibrational temperature, lower of translational.

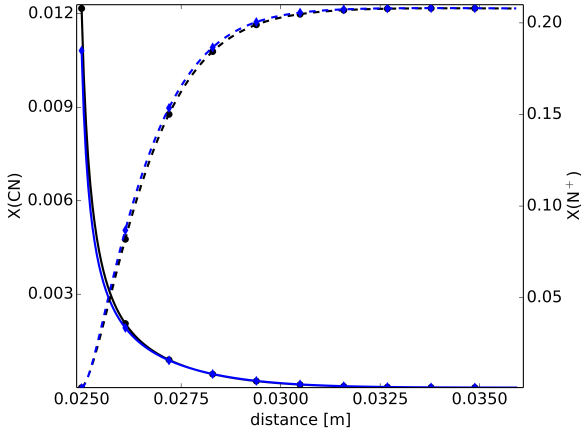

(b) CN molar fraction with solid lines. N^+ molar fraction with dashed lines.

Fig 4. CASE 2, results along the stagnation line. Surface in thermal equilibrium BC with circle marker. Surface vibrationally adiabatic with diamond markers.

Simulation surface results can be found on table 2. On the same table is also provided the temperature relative error, defined as:

$$\epsilon_S = \frac{T_S^{\mathcal{T}} - T_{S,exp}^{\mathcal{T}}}{T_{S,exp}^{\mathcal{T}}}.$$

It can be seen that the surface temperature is over-predicted when an equilibrium condition is employed, whereas the error is significantly reduced in the adiabatic case. The internal energy freezing following the use of the adiabatic condition is also in agreement with the experimentally accessed vibrational temperature within the BL, indicated with error bars in fig. 4a. The mass blowing rate is within the experimental uncertainty in both the case, being less for the adiabatic condition as a consequence of the lower surface temperature.
It follows that the surface vibrationally adiabatic BC better captures both the surface and the gas-phase features of the experimental campaign.

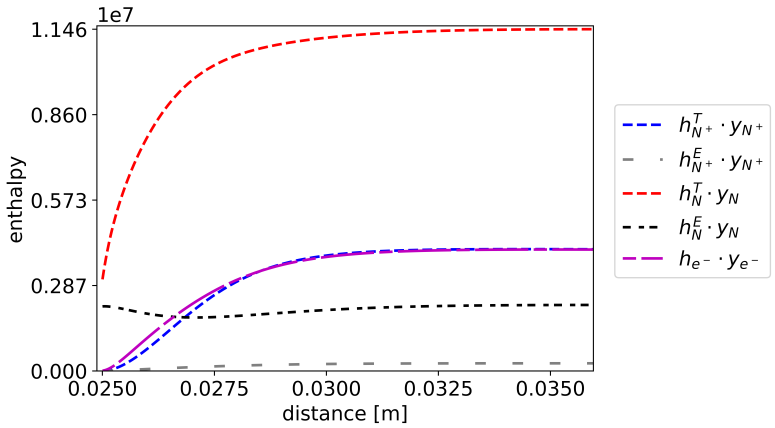

Fig 5. CASE 2, species mode enthalpy in the boundary layer.

Table 2. Surface numerical results relative to the equilibrium and adiabatic BC.

CASE	$T_{\text{equi}}^{\mathcal{T}}[K]$	$T_{\text{adi}}^{\mathcal{T}}[K]$	$\dot{m}_{\text{equi}}[g/m^2s]$	$\dot{m}_{\text{adi}}[g/m^2s]$	ϵ_{equi} [%]	ϵ_{adi}[%]
1	2440	2300	3.40	3.10	9.7	3.4
2	2530	2385	3.69	3.40	5.0	-1.0
3	2750	2575	4.29	4.00	8.5	1.6
4	2740	2571	4.30	4.05	6.4	-0.1

4.2. Sensitivity analysis on α and β parameters

In this section the results relative to the sensibility analysis performed over the α and β parameters of eq. 15 are discussed for the CASE 2, but the conclusions remain valid for all the other cases.
The translation and the vibrational temperature profile along the stagnation line for a value of $\beta = 1$ and α in [0,1] are respectively plotted in fig. 6 and fig. 7. As one could expect, these profiles are within the two above-discussed extreme cases. As before, the vibrational mode is the one affected the most: as α decreases the non-equilibrium is enhanced and for $\alpha = 0$ a condition close to the adiabatic one is achieved, restoring its already discussed non-equilibrium features. The evolution of the surface temperatures and

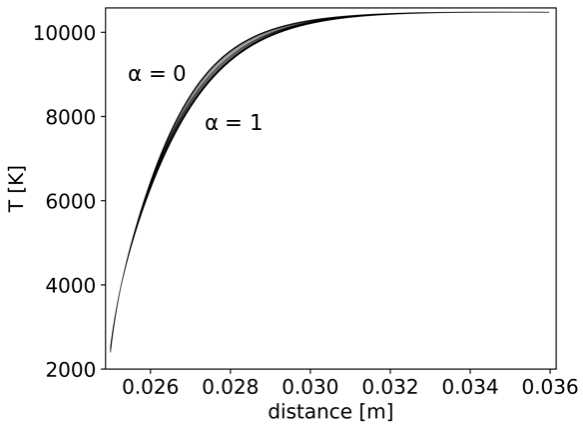

Fig 6. CASE 2, BL translational temperature distribution as function of α given $\beta = 1$.

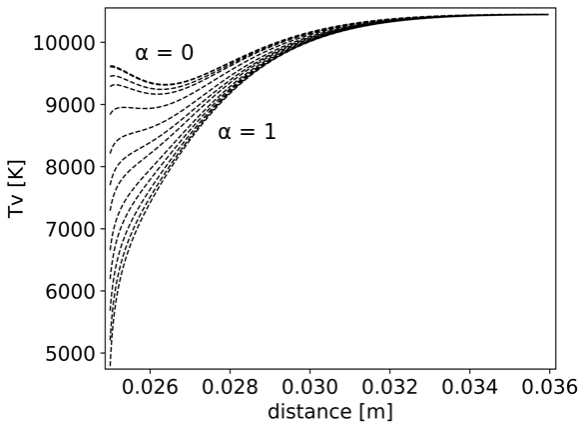

Fig 7. CASE 2, BL vibrational temperature distribution as function of α given $\beta = 1$.

of the mass blowing rate for α in [0,1] and for β equal to zero and one are respectively plotted in fig. 8 and fig. 9. The translational surface temperature decreases as α decreases and the vibrational temperature increases. This behaviour reaches a plateau for α around 10^{-3} and further reductions of α does not lead to any appreciable change in surface temperatures. The incomplete reaction energy accommodation effect is smoothed by heterogeneous quenching, and becomes more important as α decreases. Overall the boundary condition affects the translation temperature as much as 150K and the vibrational one as 5000K. It should also be remarked that even in the most favourable case, $\alpha = 1$ and $\beta = 1$, a thermal equilibrium condition cannot be obtained. Finally, the dependence of the mass blowing rate with respect to α and β parameters is plotted in fig. 9; also in this case its change is mostly due to change of surface temperature in the gamma computation and that the predicted values are inside the experimental uncertainty.

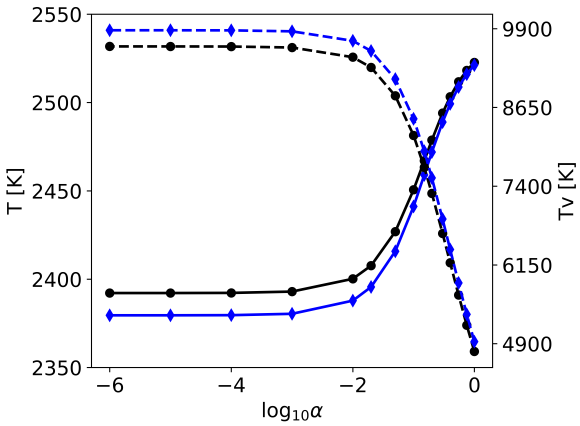

Fig 8. CASE 2. Surface translational and vibrational temperature as function of α respectively with continuous and dashed line. $\beta = 1$ with circles, $\beta = 0$ with diamond.

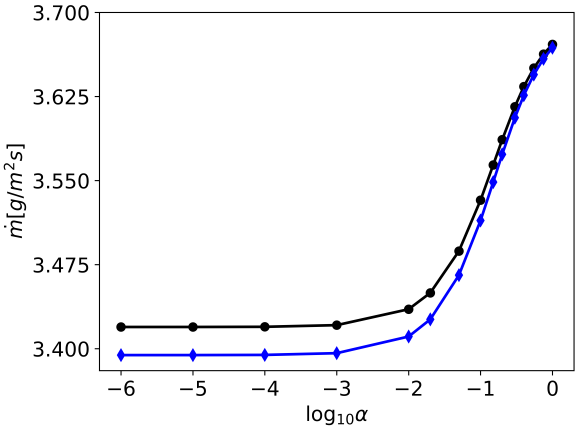

Fig 9. CASE 2. Surface blowing rate as function of α respectively with continuous and dashed line. $\beta = 1$ with cyrcles, $\beta = 0$ with diamond.

5. Conclusion

In this work, we investigated several assumptions for the closure of the vibration energy equation at the surface, namely surface in thermal equilibrium, surface vibrationally adiabatic and a novel vibrational energy balance. In the studied conditions, it was shown that an adiabatic closure can drastically reduce the error on the surface temperature prediction, suggesting that the gas-surface layer can be in thermal non-equilibrium. The source of this strong non-equilibrium was identified to be the diffusion of electronically excited atomic nitrogen inside the boundary layer. We also derived a vibrational energy surface balance and we conducted a sensitivity analysis on its parameters to access the impact on the surface temperatures prediction.

6. ACKNOWLEDGMENTS

Authors acknowledge the Air Force Office of Scientific Research (AFOSR) for supporting the work under the grant FA9550-18-1-0209.

References

[1] Peter A. Gnoffo. “PLANETARY-ENTRY GAS DYNAMICS”. In: *Annual Review of Fluid Mechanics* 31.1 (1999), pages 459–494.

[2] B. Laub and Ethiraj Venkatapathy. “Thermal protection system technology and facility needs for demanding future planetary missions”. In: *International Workshop on Planetary Probe Atmospheric Entry and Descent Trajectory Analysis and Science* (Feb. 2004), pages 239 –247.

[3] James B. Scoggins et al. “Mutation + + : MUlticomponent Thermodynamic And Transport properties for IONized gases in C++”. In: *SoftwareX* 12 (2020), page 100575.

[4] Georgios Bellas Chatzigeorgis et al. "Development of catalytic and ablative gas-surface interaction models for the simulation of reacting gas mixtures". In: *23rd AIAA Computational Fluid Dynamics Conference*. 23rd AIAA Computational Fluid Dynamics Conference. Denver, Colorado: American Institute of Aeronautics and Astronautics, 2017.

[5] Bret Halpern and Daniel E. Rosner. "Chemical energy accommodation at catalyst surfaces. Flow reactor studies of the association of nitrogen atoms on metals at high temperatures". In: *Journal of the Chemical Society, Faraday Trans. 1* 74 (Jan. 1978).

[6] Georgios Bellas-Chatzigeorgis, Paolo Barbante, and Thierry Magin. "Energy Accommodation Coefficient Calculation Methodology Using State-to-State Catalysis Applied to Hypersonic Flows". In: *AIAA Journal* 58 (Nov. 2019), pages 1–13.

[7] Bernd Helber. "Material Response Characterization of Low-density Ablators in Atmospheric Entry Plasmas". PhD thesis. Vrije Universiteit Brussel, Jan. 2016.

[8] A. Munafò and T. E. Magin. "Modeling of stagnation-line nonequilibrium flows by means of quantum based collisional models". In: *Physics of Fluids* 26.9 (2014), page 097102.

[9] Chul Park. *Nonequilibrium Hypersonic Aerothermodynamics*. Springer Berlin Heidelberg, 1990.

[10] Thierry E. Magin and Gerard Degrez. "Transport properties of partially ionized and unmagnetized plasmas". In: *Physical Review. E, Statistical Physics, Plasmas, Fluids, and Related Interdisciplinary Topics* 70.4 (Oct. 2004).

[11] Lev D. Landau. "On the theory of sound dispersion". In: *Collected Papers of L.D. Landau*. Edited by D. TER HAAR. Pergamon, 1965, pages 147 –153.

[12] Roger C. Millikan and Donald R. White. "Systematics of vibrational relaxation. J Chem. Phys, 39: 3209". In: *The Journal of Chemical Physics* 39 (Dec. 1963).

[13] Chul Park et al. "Review of chemical-kinetic problems of future NASA missions, II: Mars entries". In: *Journal of Thermophysics and Heat Transfer* 8 (Feb. 1994).

[14] Graham Candler and Robert W. Maccormack. "Computation of Weakly Ionized Hypersonic Flows in Thermochemical Nonequilibrium". In: *Journal of Thermophysics and Heat Transfer* 5 (Oct. 1991).

[15] O. Johnston Christopher. "Nonequilibrium Shock-Layer Radiative Heating for Earth and Titan Entry". PhD thesis. Virginia Polytechnic Institute and State University, Nov. 2006.

[16] Arno Klomfass, Lehr-Und Forschungsgebiet Fur Mechanik, and Siegfried Müller. "A Quasi-Onedimensional Approach for Hypersonic Stagnation-Point Flows". In: *Technical report, Internal Report* (1965).

[17] Paolo Barbante. "Accurate and Efficient Modelling of High Temperature Nonequilibrium Air Flows". PhD thesis. Politecnico di Milano, Jan. 2001.

[18] Jochen Marschall and Matthew MacLean. "Finite-Rate Surface Chemistry Model, I: Formulation and Reaction System Examples". In: *42nd AIAA Thermophysics Conference*. eprint: `https://arc.aiaa.org/doi/pdf/10.2514/6.2011-3783`. URL: `https://arc.aiaa.org/doi/abs/10.2514/6.2011-3783`.

[19] Daniele Bianchi, Alessandro Turchi, and Francesco Nasuti. "Numerical Analysis of Nozzle Flows with Finite-Rate Surface Ablation and Pyrolysis-Gas Injection". In: *47th AIAA/ASME/SAE/ASEE Joint Propulsion Conference and Exhibit*. July 2011.

[20] David Olynick, Y.-K Chen, and Michael E. Tauber. "Aerothermodynamics of the Stardust Sample Return Capsule". In: *Journal of Spacecraft and Rockets - J SPACECRAFT ROCKET* 36 (May 1999), pages 442–462.

[21] Bernd Helber, Alessandro Turchi, and Thierry E. Magin. "Determination of active nitridation reaction efficiency of graphite in inductively coupled plasma flows". In: *Carbon* 125 (Dec. 2017), pages 582–594.